IFSCC 2025 full paper (228)

# Development of Hyaluronic Acid-Lecithin Complex that Accumulates in the Stratum Corneum and Exerts Excellent Softening Effects

**Takashi Oka [1], Miyuki Saito [1], Mika Yoshimura Fujii [1], Anna Okishima [1], and Shotaro Mori [2]**

[1] MIRAI Technology Institute, Shiseido Co., Ltd., Yokohama, Japan; [2] Brand Value R&D Institute, Shiseido Co., Ltd., Yokohama, Japan

## 1. Introduction

The stratum corneum (SC) is the skin's outermost layer, serving as a hydrophobic barrier against the ingress of foreign substances and leakage of biological components [1]. The SC contains natural moisturizing factors that not only promote skin hydration but also influence skin texture, wrinkle formation, and overall appearance [2]. Thus, retaining effective ingredients such as moisturizers inside the SC is essential for maintaining healthy and beautiful skin. Known for its excellent moisturizing properties, hyaluronic acid (HA) is a biopolymer derived from vitreous humor and synovial fluid, exhibiting high viscoelasticity and water retention [3,4]. Its physiological functions, such as anti-inflammatory activity and cell proliferation promotion, vary with molecular weight. In particular, high-molecular-weight HA offers especially superior moisturizing effects. HA's skin function has been enhanced by adding hydrophobic moieties to high-molecular-weight HA [5], which increased the adsorption affinity of HA for hydrophobic SC. However, derivatization, a common method for adding functional groups, generates new chemical compounds and can reduce inherent functions [6,7].

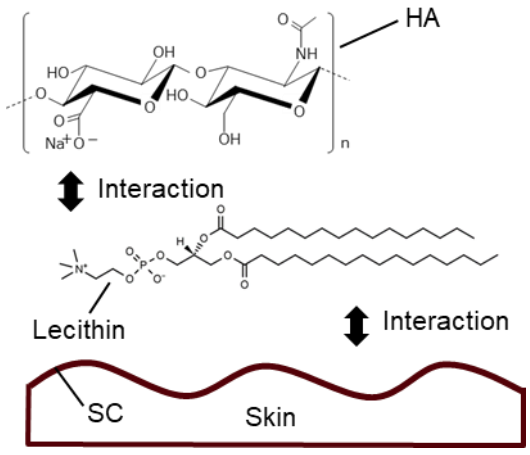


**Figure 1.** Conceptual diagram of the HA–lecithin complex. HA, hyaluronic acid; SC, stratum corneum.

Recent consumer trends show a growing preference for natural materials over synthetic products, prompting us to explore methods for imparting hydrophobicity to HA without derivatization. Known for its excellent safety profile, lecithin is primarily composed of phosphatidylcholine, a biocompatible component of biological membranes [8]. We hypothesized that lecithin could complex with HA through ionic interactions, imparting new functionalities to HA (Figure 1). Furthermore, owing to the hydrophobic groups of lecithin, complexation may enhance the affinity of HA for the SC. In this study, we successfully prepared a novel HA–lecithin complex by promoting complexation.

Specifically, we harnessed the excellent solubility of lecithin in the presence of 1,3-butylene glycol to promote the formation of a stable HA–lecithin complex through liquid–liquid mixing, which was expected to facilitate homogeneous interactions among solute molecules. This complex represents an innovative formulation that imparts new functionalities to HA without the need for derivatization. Moreover, we found that HA complexed with a small amount of lecithin had a remarkable effect on the flexibility of the SC. The enhanced affinity of HA for the SC achieved through this technology facilitated its adsorption onto the SC. Additionally, panel testing indicated that a lotion containing the complex provided superior moisturizing effects and improved the skin texture.

## 2. Materials and Methods

### 2.1 Materials

Sodium hyaluronate with an average molecular weight of 1100–1600 kDa (HA) and hydrogenated lecithin (LECI) were used to form the HA–LECI complex. 5-Aminofluorescein (FA), sodium fluorescein (FNa), and acridine orange (AO) were used for fluorescent labeling of HA or LECI. Deionized water or purified water was used as the solvent in all experiments. Unless otherwise specified, all other materials were used without purification.

### 2.2 Preparation of HA–LECI complex

An aqueous solution of 0.3 wt% HA was heated to 80 °C, to which a solution of 0.1 wt% LECI-containing 1,3-butylene glycol (1,3-BG) was added in the weight ratio of 9:1 (HA/LECI). The mixture was stirred and cooled to room temperature to obtain a dispersion of the HA–LECI complex. To observe particles of the complex, three types of fluorescently labeled complexes were prepared. First, FA-labeled HA was prepared using conventional methods [9]; this FA-labeled HA, instead of HA, was used to prepare the fluorescently labeled complex, following the same procedure described above. Second, a dispersion of the complex and a solution of AO were mixed and stirred for 24 h to prepare the complex with AO-labeled HA [10,11]. Third, a dispersion of the complex and a solution of FNa were mixed and stirred for 24 h to prepare the complex with FNa-labeled LECI [12]. The three types of fluorescently labeled complexes were thoroughly purified by dialysis through solvent exchange.

### 2.3 Morphological observation of the complex

Particles of the complex were observed under an optical microscope (BX53, Olympus, Tokyo, Japan) equipped with a fluorescence filter. In addition, cryogenic transmission electron microscopy (cryo-TEM) was conducted to confirm the morphology of the complex in solution. Specifically, the samples were thinly sectioned using an ethane rapid freezing device (EM-GP2, Leica Microsystems, Wetzlar, Germany). Subsequently, the sample was observed under a multifunctional analytical transmission electron microscope (JEM-F200, JEOL, Tokyo, Japan) at a pressure voltage of 200 kV while it was maintained in the frozen state, allowing for the observation of fine structures of the complex in solution.

### 2.4 NMR and ATR-FTIR measurements

The interactions between HA and LECI in the complex were investigated using solid-state $^{13}$C-nuclear magnetic resonance ($^{13}$C-NMR) and attenuated total reflection Fourier-transform infrared (ATR-FTIR). A dispersion of the complex was freeze-dried to prepare a coating film, and solid-state $^{13}$C-NMR spectra of the film were acquired on a spectrometer (JNM-ECA600,

JEOL). Human SC sheets were prepared using the thermal trypsin treatment method [13]. A sample of the complex was uniformly applied to the SC, which was allowed to stand at room temperature overnight to facilitate sample penetration into the SC. ATR-FTIR spectra of the SC before and after sample application were acquired on an FT-IR instrument (6700, Nicolet, Thermo Fisher Scientific, Waltham, MA, USA).

### 2.5 Contact angle of the complex in solution on the SC

Contact angles were measured to evaluate the affinity of the complex for the SC. Human SC was cast on a glass plate prepared in advance, and the contact angle of a sample of the complex on the human SC was measured using a contact angle meter (DM-501, Kyowa Interface Science, Niiza, Japan).

### 2.6 Adsorption of HA to the SC

The adsorption of HA in the complex to the SC was evaluated as follows. A sample (1 $cm^2$) of human SC was placed in a Teflon dish, and a test sample containing HA (2 $\mu L/cm^2$) was applied to the SC. After 8 h at room temperature, the surface was wiped 5 times with a soap bubble-coated cotton swab, followed by 5 wipes with purified water and one final wipe with a dry cotton swab. The SC was then immersed in 1 mL of 5 wt% methanol in Dulbecco's phosphate-buffered saline (-) (D-PBS) and ultrasonicated for 15 min to extract adsorbed HA, which was quantified using the ELISA method.

### 2.7 Skin penetration profile of HA in the complex

Excised human skin was mounted in a diffusion cell array system (Introtec, Kanagawa, Japan) with 2 mL of D-PBS applied as the receiver solution [14]. After adjusting the temperature to 32 °C and allowing the skin to hydrate for 1 h, a sample of the complex was applied at a dosage of 10 $\mu L/cm^2$ to initiate the test. Penetration was assessed at 2, 4, and 8 h. The SC surface was washed 5 times with soap bubbles and 5 times with purified water, and the SC was stripped 20 times using tape stripping discs (D101, Clinical & Derm, DAL, US). Then, the discs were immersed in 5 wt% methanol in D-PBS and ultrasonicated for 15 min. Extracted HA was quantified using the ELISA method with the HA quantification kit. This experiment was approved by our company's research ethics committee.

### 2.8 Dynamic viscoelasticity of the SC

The effects of the complex on the physical properties of the SC were determined by evaluating the dynamic viscoelasticity of the SC using a dynamic viscoelasticity measuring instrument (DVA-220, IT Measurement & Control, Osaka, Japan) [14]. A sample of human SC (3 × 20 mm) was held horizontally between 2 clamps under controlled conditions (temperature of 32 $^oC$ and relative humidity of 50%). A fixed amplitude sinusoidal stress (strain 0.2%, 1 Hz) was applied from one clamp, and the transmitted stress signal was detected using a high-sensitivity sensor installed on the other clamp. The dynamic storage modulus ($E'$) was calculated from the detected stress signal. A test solution (4 $\mu L/cm^2$) was applied to each sample, and $E'$ was measured 24 h later to assess the influence of the test solution.

### *2.9 In vivo* effect of the complex on human skin

The panel consisted of 48 healthy women aged 30 to 59 years who washed their faces with soap. The entire panel was divided into 2 groups of 24 participants to allocate the test samples. After the participants acclimatized in a constant temperature and humidity room (21±1 °C, 50%±5% RH) for 20 min, their bare skin was measured to obtain a baseline using the device corresponding to each item: skin magnification image acquisition, SC moisture content measured with a skin conductance device (SKICON-200EX and Corneometer), trans-epidermal water loss (TEWL) measured with a Tewameter, skin viscoelasticity measured with a Cutometer, and replica of the skin surface. Among the 4 types of test samples (Table 1), 2 samples (0.5 mL each) were allocated to each group, and participants applied the samples to one-half of their faces centered on the cheeks, twice daily for 4 weeks. Skin measurements similar to those conducted to obtain the baseline were performed 2 and 4 weeks after sample application. This panel testing was approved by our company's research ethics committee, and written informed consent was obtained prior to testing.

**Table 1.** Formulation of test samples

| | Lotion with the complex | Base lotion | Lotion with HA only | Lotion with LECI only |
|---|---|---|---|---|
| Water | 80.99 | 81.27 | 81 | 81.26 |
| Ethanol | 3 | 3 | 3 | 3 |
| Glycerol | 5 | 5 | 5 | 5 |
| 1,3-BG | 8 | 8 | 8 | 8 |
| Dipropylene glycol | 2 | 2 | 2 | 2 |
| HA | 0.27 | - | 0.27 | - |
| LECI | 0.01 | - | - | 0.01 |
| Polyoxyethylene hydrogenated castor oil | 0.1 | 0.1 | 0.1 | 0.1 |
| Lactic acid | 0.01 | 0.01 | 0.01 | 0.01 |
| 50wt% sodium lactate aq. | 0.09 | 0.09 | 0.09 | 0.09 |
| Tetrahydroxypropyl ethylenediamine | 0.03 | 0.03 | 0.03 | 0.03 |
| Phenoxyethanol | 0.5 | 0.5 | 0.5 | 0.5 |
| Total | 100 | 100 | 100 | 100 |

### 2.10 Statistical analysis

Statistical analysis was performed using the Statcel4 add-in for Excel. The presented *p*-values were obtained from the Tukey–Kramer multiple comparison test. Comparisons between the two groups were conducted using Student's t-test.

## 3. Results

### 3.1 Microscopic observation of the complex

Figure 2(a) presents an optical microscopy image of the particles of the complex. Although submicron-sized particles were predominant, larger particles (marked by arrows), several μm in size, with a more discernible shape were also present.

Fluorescence microscopy images were acquired to estimate the location of anionic HA in particles of the complex. Figure 2(b) shows an enlarged fluorescence microscopy image of the complex with FA–HA. The strong fluorescence observed around the particle indicated that HA was predominantly distributed on the surface of particles of the complex. Fluorescence images of the complex labeled with cationic AO were similar. Fluorescence microscopy

images were also acquired to estimate the location of LECI in particles of the complex. Figure 2(c) shows an enlarged fluorescence microscopy image of the complex with FNa-labeled LECI. The fluorescence images of LECI only particles labeled with FNa were similar, suggesting that LECI was predominantly distributed in the core of particles of the complex.

Figure 2(d) presents a cryo-TEM image of particles of the complex. A bright band surrounded the dark core with a diameter of approximately 50 to 100 nm (marked by arrows). These results, in conjunction with the aforementioned fluorescence microscopy images, indicated that the dark core consisted of LECI, while the surrounding bright band was composed of HA. This finding confirmed the presence of particles of the complex in the liquid.

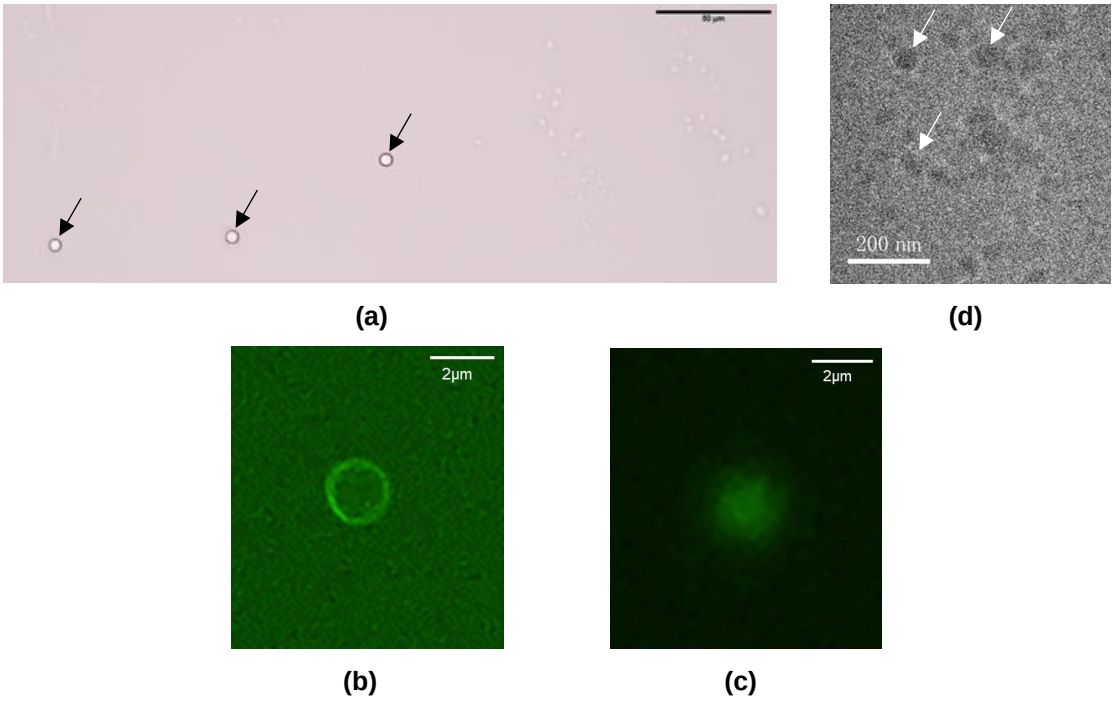


**Figure 2. (a)** Optical microscopy images of particles of the complex (scale bar = 50 μm). **(b, c)** Enlarged fluorescence microscopy images of the complex with FA-labeled HA (b, scale bar = 2 μm) or FNa-labeled LECI (c, scale bar = 2 μm). **(d)** Cryo-TEM image of the complex (scale bar = 200 nm).

### 3.2 NMR and ATR-FTIR measurements

Figure 3(a) and (b) shows the solid-state $^{13}$C-NMR spectra of the complex and each individual component (LECI or HA). The peaks centered at 54.5 and 174.0 ppm corresponded to the trimethylammonium group of LECI and the carboxyl group of HA, respectively. Upon complexation, the former peak slightly shifted toward the low magnetic field side, whereas the latter peak slightly shifted toward the high magnetic field side, suggesting that weak ionic interactions occurred between HA and LECI inside the complex, which likely drove the complexation (marked by arrows). Figure 3(c) shows the ATR-FTIR spectra of the SC with and without the application of the complex. The characteristic peaks of the hydrocarbon groups of the untreated SC slightly shifted to lower wavenumbers upon the application of the complex (marked by arrows), suggesting that weak hydrophobic interactions occured between the SC and LECI, rather than HA, in the complex because of the absence of hydrophobic groups in HA.

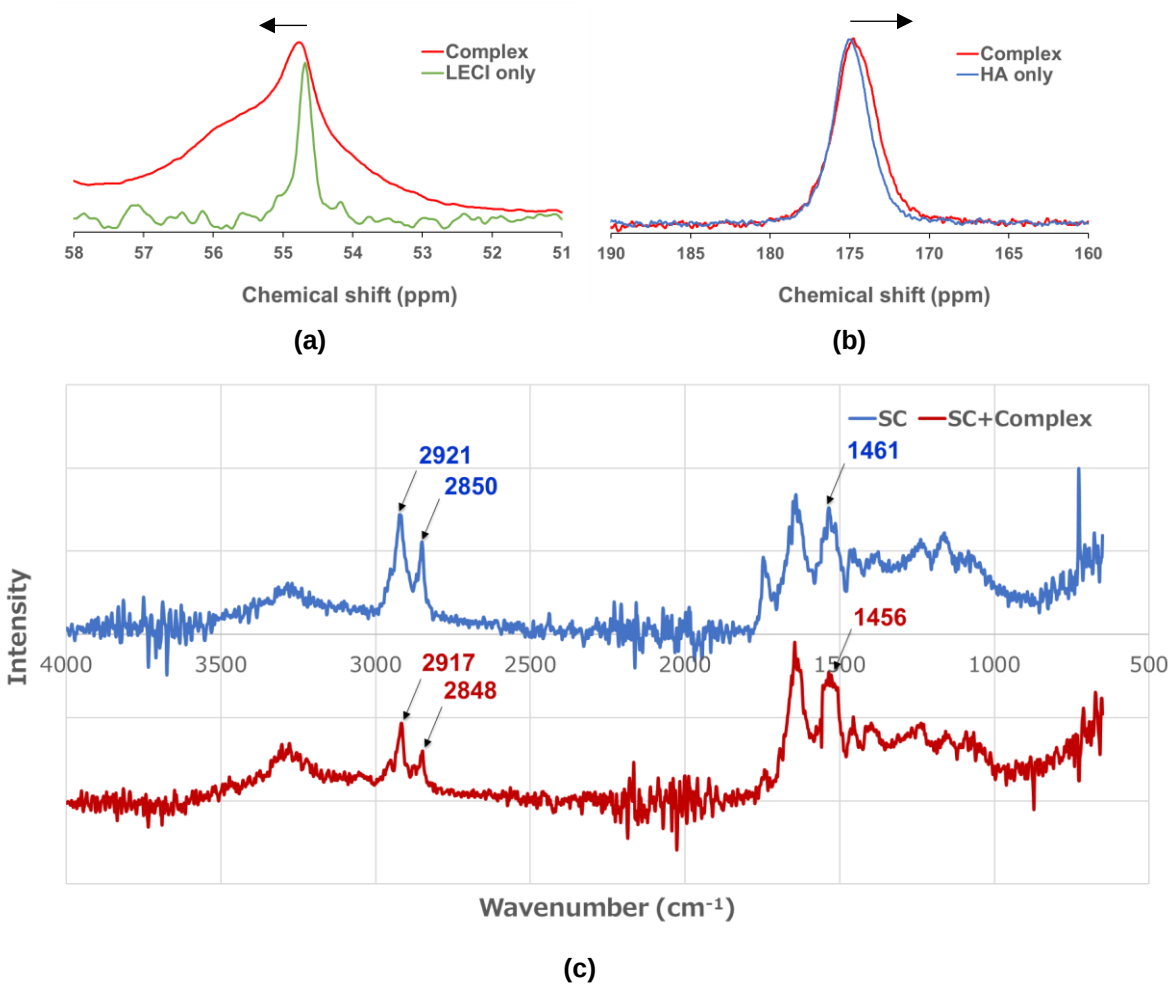


**Figure 3. (a, b)** Solid-state $^{13}$C-NMR spectra of the complex (a, b) and constituents, LECI (a) and HA (b). **(c)** ATR-FTIR spectra of the SC with and without the application of the complex.

### 3.3 Contact angles to the SC and adsorption of HA onto the SC

Figure 4(a) shows the contact angles of the complex and its components on the SC. The contact angle of 10 wt% aqueous 1,3-BG on the SC did not change significantly upon the addition of HA or LECI to the aqueous solution of 1,3-BG. However, the contact angle of the HA–LECI complex on the SC was significantly reduced compared with the components of the complex.

Figure 4(b) shows the amount of HA adsorbed onto the SC. The test sample was applied on the SC, and after 8 h, the average amount of HA in the SC was determined. Compared with HA only, HA in the complex was adsorbed on the SC in a significantly greater amount. This result suggests that the affinity of HA for the SC was enhanced by complexation with LECI.

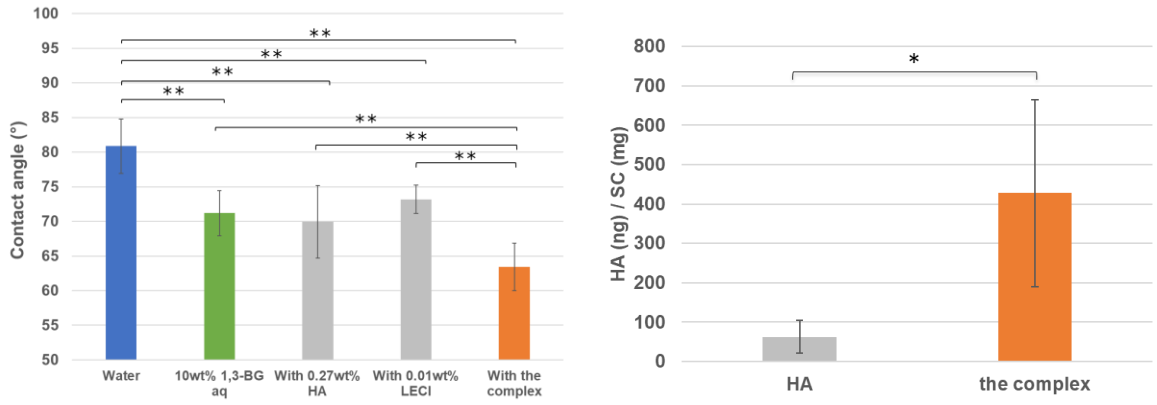


**Figure 4**. **(a)** Contact angles of each sample on the SC. Values are expressed as mean ± S.D. ($n$=10), **$p$<0.01, Tukey's test. **(b)** Amount of HA adsorbed on the SC. Values are expressed as mean ± S.D. ($n$=3), *$p$<0.05, Student's t-test.

### 3.4 HA penetration into the SC

Figure 5 shows the amount of HA (with and without LECI) penetrating the SC over time. The results showed that HA penetration was slightly enhanced by complexing HA with LECI, although the improvement was not statistically significant.

### 3.5 Viscoelasticity of the SC

Figure 6 shows viscoelasticity of the SC (Figure 6) determined following the application of different lotions (Table 1). Compared with the base lotion, neither the lotion with HA nor the lotion with LECI exhibited a softening effect on the SC. However, the lotion with the HA–LECI complex had an excellent softening effect on the SC.

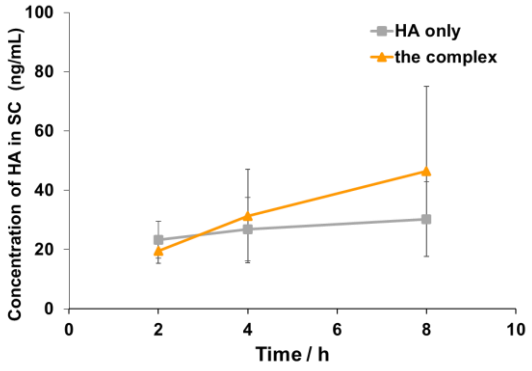


**Figure 5**. Comparison of HA (with and without LECI) adsorption on the SC. Values are expressed as mean ± S.D. ($n$=4), n.s., Student's t-test.

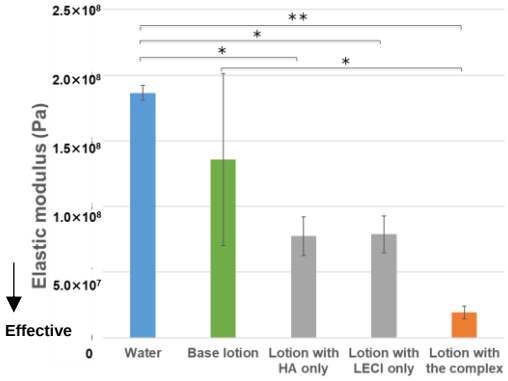


**Figure 6**. Effect of lotion formulation on the viscoelasticity of the SC. Values are expressed as mean ± S.D. ($n$=3), *$p$<0.05, **$p$<0.01, Tukey's test.

### 3.6 *In vivo* effect of the complex on human skin

Figure 7(a) presents the measured water content of the surface layer of the SC. A higher water content indicates a superior moisturizing effect of the applied lotion. The results revealed that

the coexistence of HA with LECI through complexation enhanced the moisturizing effect of the lotion in the upper layer of the SC. Figure 7(b) shows the score of the skin texture obtained from the skin replica analysis. The score serves as an indicator of the anisotropy calculated from the number of skin grooves in both vertical and horizontal directions, with lower values indicating a more organized skin texture. The results similarly revealed that using the lotion with the HA–LECI complex significantly improved the skin texture. Moreover, continuous use of the lotion with the complex had a significant effect on skin texture (Figure 7(c) and (d)). Over time, skin surface ridges and grooves became more pronounced. However, the TEWL and skin viscoelasticity revealed that applying the complex did not produce any significant effect on the deeper layers of the skin.

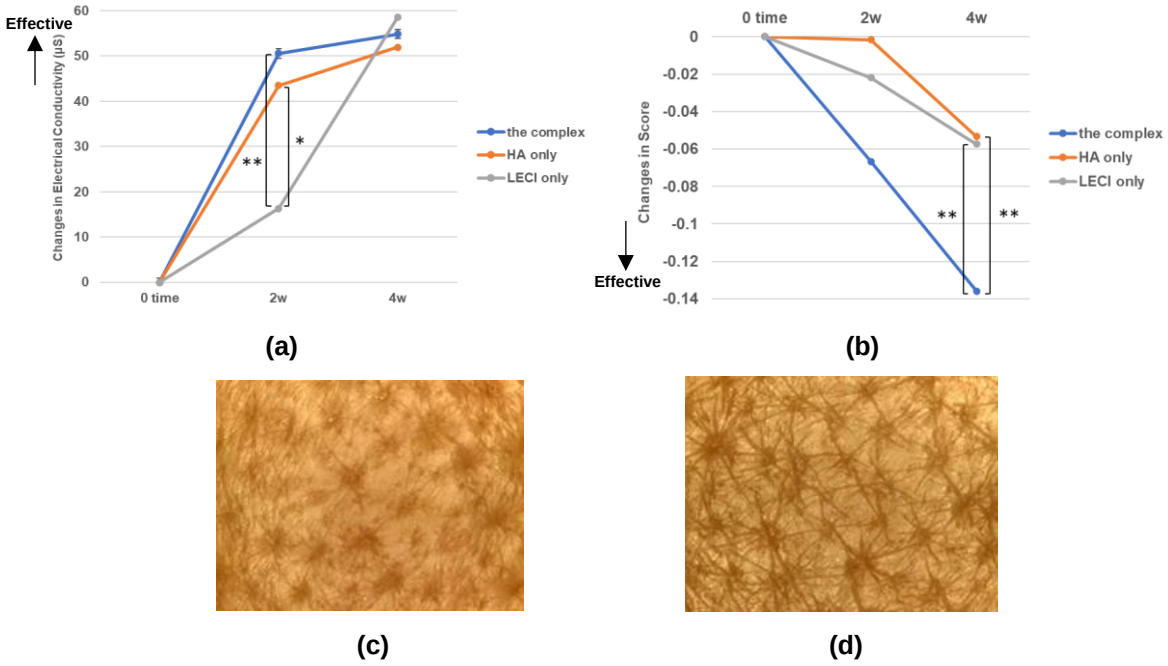


**Figure 7. (a)** Moisturizing effect of lotions assessed by evaluating the skin water content. Values are expressed as mean ± S.D. ($n$=24), *$p$<0.05, **$p$<0.01, Tukey's test. **(b)** Score of skin texture. Values are expressed as mean ± S.D. ($n$=24), **$p$<0.01, Tukey's test. **(c, d)** Images of skin texture before using the lotion with the complex (c) and after 4 weeks of continuous use of the lotion with the complex (d).

## 4. Discussion

### 4.1 Formation of HA–LECI complex

HA has been functionalized through non-derivatization methods, such as formulation with salts [14] and complexation with polyions [15]. However, these studies were focused on enhancing the skin penetration of HA, and in the latter route, HA remains complexed with the polyion in the skin, which is thought to inhibit the inherent moisturizing effects of HA. Here, we aimed to develop a smart formulation that would promote the moisturizing effects of HA. For this reason, we complexed HA with LECI, which was expected to exhibit stimuli-responsive properties while synergistically enhancing the moisturizing effects of HA. Microscopy investigations of the complexation of HA with LECI provided intriguing findings. Fluorescence microscopy images revealed that particles of the complex were formed with a significant distribution of HA around lecithin particles. Additionally, cryo-TEM images indicated that particles of the complex

existed in solution. Furthermore, NMR spectra suggested that ionic interactions between the carboxyl groups of HA and the trimethylammonium groups of LECI were likely the driving force of the complexation.

### 4.2 Adsorption of HA–LECI complex in the SC and effects on skin

ATR-FTIR spectra suggested that weak hydrophobic interactions occurred between LECI and the SC. Charge repulsion between LECI molecules and HA molecules was likely suppressed through ionic interactions, which facilitated hydrophobic interactions between LECI and the SC. Consequently, the amount of HA adsorbed onto the SC increased. On the basis of these considerations, we conceived a predictive model for SC adsorption and moisturizing, as presented in Figure 8. Although HA has excellent moisturizing properties, when used alone, its affinity for the SC is low, limiting moisture retention in the upper layers of the SC. In contrast, the HA–LECI complex significantly enhanced the affinity of HA for the SC, notably increasing the amount of HA retained in the upper layers of the SC. As a result, the complex provides superior SC softening effects. Furthermore, the panel testing revealed that the synergistic effect of HA and LECI significantly improved the moisturizing effect and skin texture in the upper layers of the SC, with these effects becoming more pronounced with continued use. One possible reason for this is that lecithin, which has a high affinity for biological membranes, may contribute to the uniform distribution of moisture-retained HA in the upper SC, leading to a marked improvement in skin texture. In the field of aesthetic medicine, techniques exist for injecting HA to improve the volume of the deeper layers of the skin [16–18]. However, the complexation method described here is expected to enable approaches and improvements to the skin's surface layer that cannot be achieved with traditional esthetic medical methods. Additionally, the HA–LECI complex offers substantial advantages in terms of ease of use, because consumers can easily apply it. Moreover, the complex effectively improves skin hydration and texture with short-term repeated use.

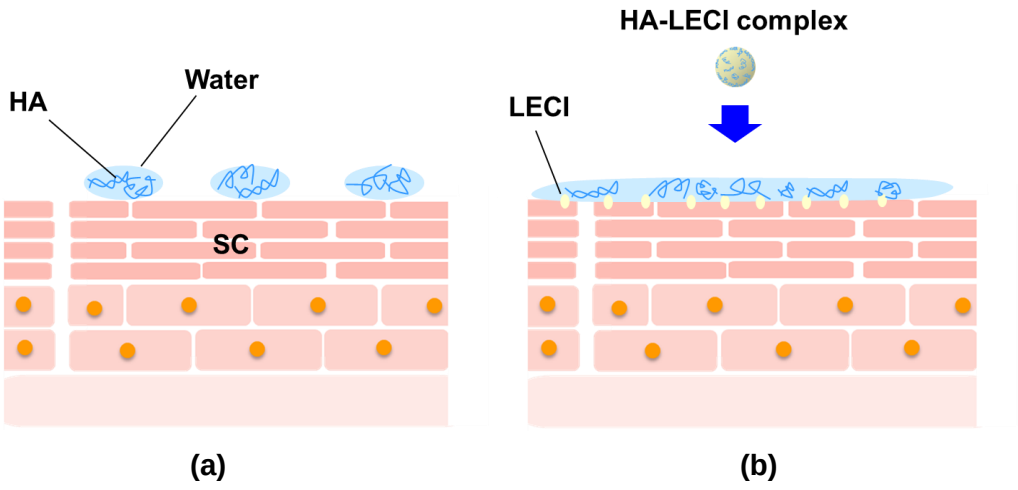


**Figure 8.** Proposed model for predicting HA adsorption and moisturizing of the SC in the case of **(a)** HA only and **(b)** the complex. HA, hyaluronic acid; LECI, lecithin; SC stratum corneum.

## 5. Conclusion

Investigation of the HA–LECI complex revealed the following findings. HA was complexed with LECI *via* ionic interactions, which imparted hydrophobicity to HA without the use of chemical modification owing to the amphiphilicity of LECI. The complex exhibited an increased affinity for the SC, enhancing the adsorption of HA on the SC, which contributed to its excellent softening effect on the skin. Continuous use of a lotion formulated with this complex provided superior moisturizing effects and improved the skin texture. Notably, this complex is composed entirely of naturally derived ingredients and offers excellent skin benefits. Therefore, the complex, in use, is expected to provide not only assurance to a wide range of consumers, including those with a preference for natural products, but also confidence in their bare skin.

## Acknowledgments

We would like to thank Ms. Hiroko Ichiwata, Ms. Ayano Nakamura, and Dr. Kazuyuki Miyazawa for useful discussions. We are also grateful to Mr. Tadao Fukuhara for NMR measurements, Ms. Kaori Ikuta, Mr. Yohei Takahashi, and Mr. Norinobu Yoshikawa for TEM observations, and Ms. Megumi Mizugaki and. Ms. Miho Yajima for support with *in vivo* panel testing. We thank Edanz (https://jp.edanz.com/ac) for editing a draft of this manuscript.

## Conflict of Interest Statement

NONE.

## References

1. I. H. Blank, *J. Invest. Dermatol.*, 18: 433–440 (1952).
2. K. Laden and R. Spitzer, *J. Soc. Cosmet. Chem.*, 18: 351–360 (1967).
3. A. R. C. Salih, H. M. U. Farooqi, H. Amin *et al.*, *Future J. Pharm. Sci.*, 10: 63 (2024).
4. G. Abatangelo, V. Vindigni, G. Avruscio *et al.*, *Cells*, 9: 1743 (2020.)
5. T. Oka, M. Uemura, N. Ueno *et al.*, *J. Cosmet. Sci.*, 50 : 171–184 (1999).
6. C. E. Schanté, G. Zuber, C. Herlin, T. F. Vandamme, *Carbohydr. Polym.*, 85: 469–489 (2011).
7. H. Kim, H. Jeong, S. Han *et al.*, *Biomater.*, 123: 155–171 (2017).
8. D. J. Canty and S. H. Zeisel, *Nutr. Rev.*, 52: 327–339 (1994).
9. A. Ogano *et al.*, *Carbohydr. Res.*, 105: 69–85 (1982).
10. F. Mravec *et al.*, *Adv. Planar Lipid Bilayers Liposomes*, 14: 235–255 (2011).
11. J. Mondek, F. Mravec, T. Halasová *et al.*, *Langmuir*, 30: 8726–8734 (2014).
12. H. Mochizuki, M. Yamada, S. Hato *et al.*, *Br. J. Ophthalmol.*, 92: 108–111 (2008).
13. A. M. Kilgman and E. Christophers, *Arch. Dermatol.*, 88: 702–705 (1963).
14. M. Y. Fujii, A. Okishima, H. S. Ichiwata *et al.*, *Sci. Rep.*, 13: 10782 (2023).
15. M. Shigefuji and Y. Tokudome, *Materialia*, 14: 100879 (2020).
16. J. Kim, *Arch. Aesthetic Plast. Surg.*, 20: 97–103 (2014).
17. B. Bravo *et al.*, *Dermatol. Ther.*, 35: e15903 (2022).
18. H. Cheng, Y. Chen, M. Wang *et al.*, *J. Cosmet. Laser Ther.*, 20: 454–461 (2018).